

Characterization of Multiferroic Thin Films Generated with Molecular Beam Epitaxy

Margaret Anderson

California Institute of Technology

*REU Program: 2017 Platform for the Accelerated Realization, Analysis, and Discovery of Interface Materials
Research Experience for Undergraduates (PARADIM REU) Program with Caltech SURF*

*PARADIM REU Principal Investigator: Darrell Schlom, PARADIM Director,
Materials Science and Engineering, Cornell University*

PARADIM REU Mentor: Rachel Steinhardt, Materials Science and Engineering, Cornell University

REU Caltech Co-Mentor: Katherine Faber, Materials Science, California Institute of Technology

Primary Sources of PARADIM REU Funding: NSF Materials Innovation Platform Program, Grant # DMR-1539918;

Caltech Student-Faculty Programs Summer Undergraduate Research Fellowship (SURF)

Contact: maanders@caltech.edu, ds636@cornell.edu, rs963@cornell.edu

Website: http://www.cnf.cornell.edu/cnf_2017reu.html

Abstract:

Magnetoelectric multiferroic thin films exhibit coupled ferromagnetism and ferroelectricity. Interest in these multiferroics stems from their potential applications in spin-based computing and novel information storage methods. Through characterization with x-ray diffraction (XRD), atomic force microscopy (AFM), and vibrating sample magnetometry (VSM), the growth of multiferroic films with molecular beam epitaxy (MBE) was optimized. Both strain-coupled $\text{Fe}_x\text{Ga}_{1-x}$ composites and rare earth ferrite superlattices were studied. Additionally, this study searched for compatible bottom electrodes that facilitate the measurement of the ferroelectric properties of the films. Because the electrodes are necessarily located between the substrate and the film, all three must have compatible crystal lattice parameters in order to grow successfully with MBE. Characterization of the electrodes with XRD omega rocking curves and AFM revealed that PIN-PMN-PT produced slightly better iridium electrodes and $\text{Fe}_x\text{Ga}_{1-x}$ films than PMN-PT.

Methods:

X-ray Diffraction. X-ray diffraction was conducted with a Rigaku Smartlab X-ray Diffractometer with a Ge 220 monochromator on the incident side in a parallel beam (PB) configuration. Samples were placed on misoriented single crystal silicon during scanning to limit the background signal — θ - 2θ scans were used to verify composition, phase, and orientation of the epitaxial thin films. Based on Bragg's law, x-rays incident on the crystalline sample at a Bragg angle (determined by the presence and separation of crystal planes within the material) diffract with a relative displacement equal to an integer multiple of their wavelength. As a result, the x-rays interact with constructive interference, producing a peak in a θ - 2θ scan at the Bragg angle — ω -rocking curves gave a measure of structural crystal quality. By 'rocking' the incident angle of the x-rays near a Bragg angle in XRD, the width of a peak can give an indication of the quality of the crystal. If the crystal was absolutely perfect, the rocking curve would have a FWHM of nearly 0 degrees. The only angle that would satisfy Bragg's law and diffract x-rays would be the exact Bragg angle. However, defects within the crystal introduce slight changes in the orientation of the crystal planes and diffract x-rays at angles slightly off from the exact Bragg angle of a theoretically pure crystal, thereby widening the peak. Therefore, by performing rocking curve measurements, the structural quality of crystal samples can be determined by the FWHM of the resulting peak.

Atomic Force Microscopy. An Asylum Research MFP-3D scanning probe microscope system in AC tapping mode was used to evaluate the surface quality of samples. AFM uses the change in amplitude of a harmonically oscillating cantilever to map the surface features of a sample. The calculated height of the sample at each position is represented as a colored pixel and arranged spatially to produce an image of the surface. RMS surface roughness, a measure of the average deviation of the film surface from a perfectly flat plane, was used to evaluate the smoothness of film growth.

Vibrating Sample Magnetometry. A 9T Quantum Design Physical Property Measurement System (PPMS) with a vibrating sample magnetometer was used to evaluate the magnetic properties of $\text{Fe}_x\text{Ga}_{1-x}$ thin films. Measurements were conducted at room temperature. By oscillating the sample in a sweeping external magnetic field, a hysteresis loop characteristic of ferromagnetic materials was generated. The raw data was the summation of the magnetic signal from both the sample and the diamagnetic substrate. The result is the sloped loop shown below in Figure 1.

The diamagnetic signal from the substrate is characteristically a negatively sloped straight line. The slope of this line was determined via regression on the tails of the uncorrected hysteresis loop (Figure 2). The result was subtracted from the data. To quantify the

magnetic moment in emu/cm^3 , the data was divided by the volume of the $\text{Fe}_x\text{Ga}_{1-x}$ film, resulting in the final hysteresis loop used to describe the ferromagnetic properties of the film.

Molecular Beam Epitaxy. The samples in this study were grown by reactive-oxide molecular beam epitaxy (MBE) using a Veeco Gen 10 growth chamber. My graduate student mentor, Rachel Steinhardt, grew all of the films characterized here because the complex method of MBE was beyond the scope of a ten-week fellowship. In MBE, pure samples of each element within the desired structure are heated within a crucible, called an effusion cell, to produce a 'beam' that is directed towards the heated substrate. The elements are deposited on the substrate, producing an epitaxial crystalline film. By varying each element's flux rate, substrate temperature, and the pressure of O_2 and ozone within the growth chamber, complex and atomically ordered crystalline films can be grown with high precision.

In order to grow high quality epitaxial crystals, the films must be grown on structurally compatible substrates. For example, lutetium ferrite has a hexagonal structure, rather than the cubic structure of many perovskites grown with MBE. Yttria-stabilized zirconium (YSZ) has a cubic structure that is generally incompatible with the hexagonal ferrites. Yet, when cut to expose the $\langle 111 \rangle$ crystallographic plane, the surface behaves hexagonally (Figure 3). Therefore YSZ $\langle 111 \rangle$ is a suitable substrate for lutetium ferrite superlattice growth.

Acknowledgments:

This work was supported by the NSF via the Platform for the Accelerated Realization, Analysis, and Discovery of Interface Materials (PARADIM) under Cooperative Agreement No. DMR-1539918, and made use of the Cornell Center for Materials Research Shared Facilities, which are supported through the NSF MRSEC program (DMR-1120296). I would like to thank Professor Darrell Schlom for his advice and kindness during this research experience. Special thanks to Rachel Steinhardt for her technical guidance and dedication to making my summer a success. I would also like to thank Professor Katherine Faber for agreeing to act as my faculty co-mentor at Caltech. Finally, I would like to thank the Caltech Student-Faculty Programs office for the opportunity to participate in the Summer Undergraduate Research Fellowship and all of the personnel at both Caltech and Cornell that offered welcome advice and assistance in my voyage across the country to have this world-class research fellowship.

Find Margaret's full Caltech report online at <http://paradim.cornell.edu/education/2017-reu-participants/>

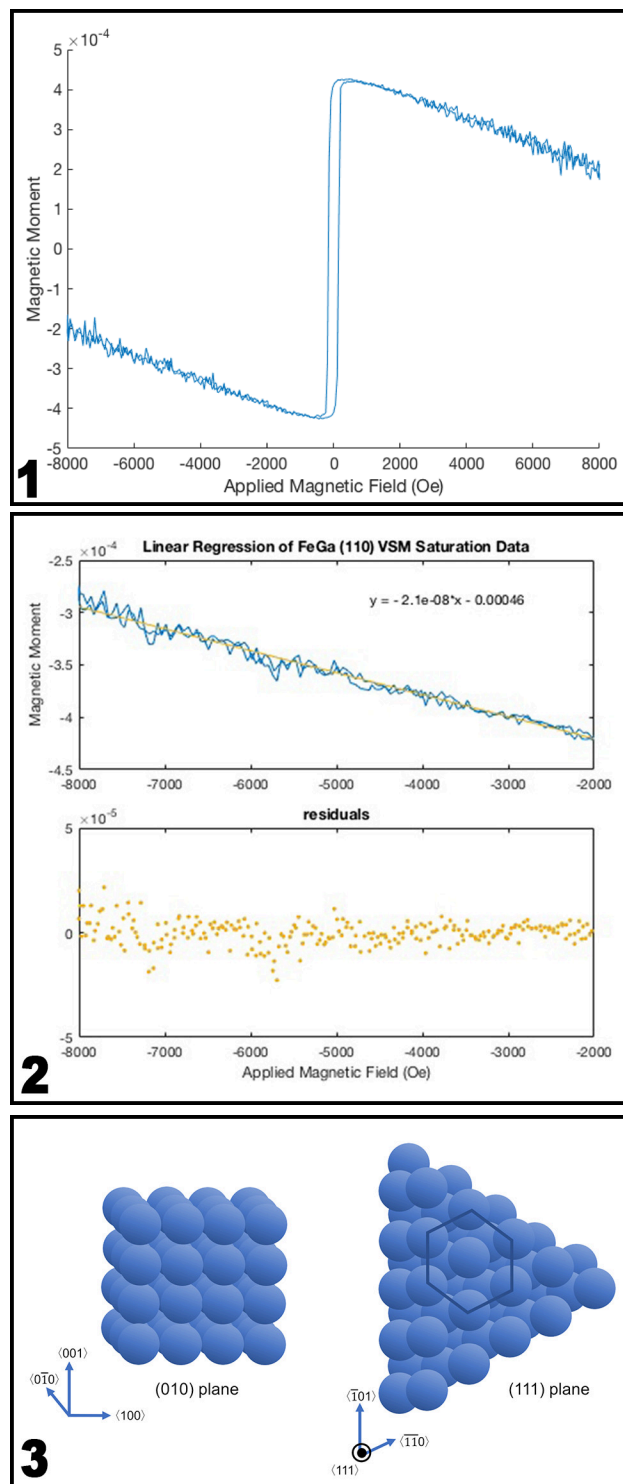


Figure 1, top: Uncorrected M vs. H hysteresis loop for an Fe_xGa_x film on PIN-PMN-PT measured in the $\langle 110 \rangle$ direction.

Figure 2, middle: Linear regression on the lower tail of $\langle 110 \rangle$ uncorrected data. Residuals show random scatter indicating that the linear model is valid. The slope of the equation in the upper graph was used as the slope of the linear diamagnetic signal subtracted from the raw data.

Figure 3, bottom: On the left is a simple cubic crystal structure. When sliced to expose the $\langle 111 \rangle$ plane, the result is a hexagonal structured surface as depicted on the right. A similar hexagonal structure is produced along the $\langle 111 \rangle$ of a face-centered cubic crystal like YSZ. Crystallographic directions are shown for reference.